Rev. Roum. Sci. Techn.– Électrotechn. et Énerg.
Vol. **70**, *3*, pp. 307–311, Bucarest, 2025

INTERVAL TYPE 2 FUZZY LOGIC CONTROL FOR BRUSHLESS DOUBLY FED INDUCTION GENERATOR BASED ON WIND ENERGY CONVERSION SYSTEMS

HELLALI LALLOUANI [1], MOUSSA OUSSAMA [2], BOUZIDI ALI [3], AKKA ALI [4]

Keywords: Brushless doubly fed induction generator (BDFIG); Wind energy conversion systems (WECS); Interval type 2 fuzzy logic control (IT2FLC); Renewable energy; Back-to-back converter; Power factor.

This paper presents a novel approach to utilizing interval type 2 fuzzy logic controllers (IT2FLC) for controlling brushless doubly fed induction generators (BDFIGs) in wind energy conversion systems (WECS). However, the complex dynamics and nonlinear characteristics of BDFIGs pose significant challenges for their control, especially under varying wind conditions. The proposed IT2FLC system design addresses these challenges by handling uncertainties and nonlinearities more effectively than traditional control methods. The interval-type 2 fuzzy logic approach offers a higher degree of freedom and improved performance in handling uncertainties, particularly in the presence of noisy or imprecise data. The IT2FLC system adapts to changing wind speeds and generator operating conditions, ensuring optimal power extraction and efficient energy conversion. The simulations demonstrate that the proposed IT2FLC system significantly enhances the performance of BDFIGs in WECS, providing stable and reliable control across various operating conditions. The system's ability to manage uncertainties and maintain efficient operation makes it a promising solution for integrating renewable energy sources into the grid.

1. INTRODUCTION

Wind energy is a growing renewable energy source, with an increasing number of variable-speed wind turbines. Wind turbine control systems, known as maximum power point tracking (MPPT), optimize energy conversion to maximize power production. This includes adjusting the blade pitch angle, propeller rotation speed, or even the generator's control. Although most installed wind turbines are fixed-speed, the number of variable-speed wind turbines is constantly increasing. This approach ensures optimal use of wind energy for electricity production [1]. The wind turbine continually seeks to extract maximum power, adapting to each variation in wind speed. When the wind becomes too strong, safety devices limit the power produced, preventing damage to the turbine. This system ensures maximum power extraction [2,14].

The brushless doubly fed induction generator (BDFIG) has gained significant interest due to its numerous advantages. Its rotor has a cage structure and is robust because it does not have brush-ring contact. It also allows for controlling speed and power factor, making it a 3rd-generation machine in wind power systems. The cascade of two BDFIGs is considered the first practical realization of a dual-fed brushless direct current (BDFIG) machine. The BDFIG consists of a cage rotor and a stator with two independent three-phase windings: power winding (PW) and control winding (CW) [3]. The rotor performs magnetic decoupling between the windings. A BDFIG's design necessitates a perfect ratio between the number of poles in the stator windings and the number of turns in the rotor [4].

A properly constructed BDFIG does not guarantee machine functionality; it requires a correlation between the frequency of two stator power sources and the rotor's rotational speed. BDFIG's primary characteristic is its ability to modify rotor current through the control winding. By using the rotor [5], the number of pole pairs ($P_p \neq P_c$) must differ to prevent direct magnetic coupling between the stator's two windings. To avoid dissociation, the currents must have the same spatial distribution, which affects the machine's physical structure. This requirement is met by [6,7]:

$$\omega_r = \frac{\omega_{sp}+\omega_{sc}}{P_p+P_c}, \quad N_r = P_p + P_c \,. \tag{1}$$

ω_{sp} and ω_{sc} are given as the electrical angular velocities of the power winding (PW) and control winding (CW) voltages, and w_r is the angular speed of the rotor.P_pAnd $P_c$represent the number of pole pairs of PW and CW, respectively. In this case, $P_p = 3$ and $P_c = 1$ [7,8].

The Brushless doubly-fed Induction Generator (BDFIG) is widely used in wind energy production. It uses a vector control strategy to adjust the orientation of the power winding (PW) flow. The PW flux value remains constant due to the BDFIG's constant voltage. The study of BDFIG's application in wind energy production is crucial. Vector control by flux orientation offers a solution for improved performance in variable-speed applications, particularly in brushless doubly fed induction generators. We use the orientation of the stator flux as a generator to highlight the relationships between the power stator (PW) and control stator (CW) [6–8].

The relationship between rotor signals and the machine stator allows for control of active and reactive power exchange between the machine and the network. Vector control uses classical regulators (PI), calculated from machine parameters [9,14]. These regulators are specifically designed to enhance performance. However, they are susceptible to parameter perturbations, model errors, and external perturbations, and can exhibit asymptotic convergence. They are simple to build and have low computational cost. We must design robust controls to make the brushless doubly fed induction generator insensitive to external disturbances and parametric variations, thereby achieving high performance.

Among them, fuzzy logic control. Type 2 fuzzy logic control is a form of controlling that uses fuzzy rules to identify the best response to a given input [12]. It helps account for uncertainty and imprecision in input data, which is especially important in cases where variables are

[1,3]LGE, University of Msila, University Pole, Road Bordj Bou Arreridj, Msila 28000, Algeria.
[2]Department of Automatics and Electromechanical, Faculty of Science and Technology, Université de Ghardaia, Algeria.
[4] Department of Physics Sciences, Higher Normal School of Boussada, Boussada, 28001, Algeria.
E-mails: lallouani.hellali@univ-msila.dz, moussa.oussama@univ-ghardaia.dz, bouzidi.ali@univ-msila.dz, akka_ali@ens-bousaada.dz

DOI: 10.59277/RRST-EE.2025.70.3.4

difficult to measure correctly. In summary, type 2 fuzzy logic control is a control method that considers uncertainty and imprecision in input data. When variables are challenging to measure accurately, it serves as a control method for physical systems.

The primary goal of this paper is to address issues related to the stability of most control algorithms. Our contribution to this study is to confirm the monitoring and control performance, and then to make the wind system insensitive to parametric fluctuations.

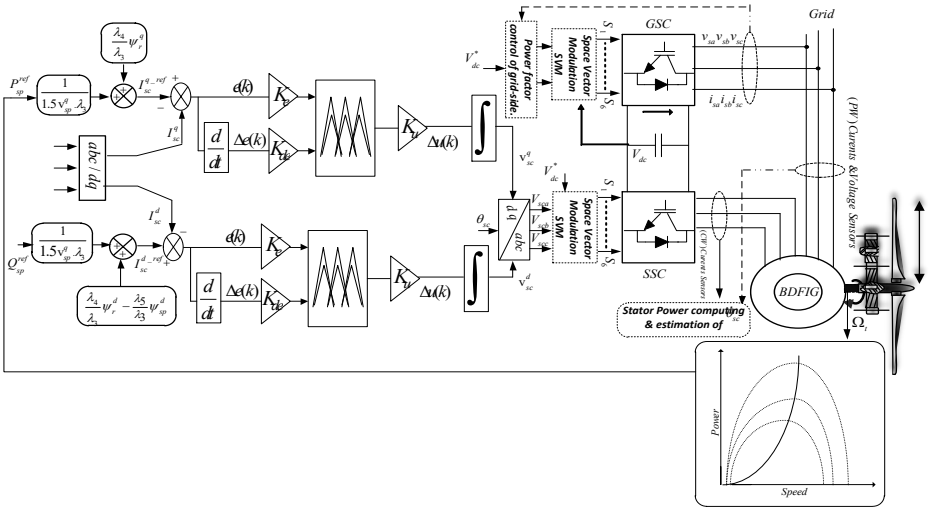

Fig. 1 – WECS based on the BDFIG.

This control technique is robust and likely to optimize wind turbine production, particularly one using a brushless double-fed asynchronous generator (BDFIG). This study aims to develop a control technique based on fuzzy logic to manage the active and reactive power generated by BDFIG, thereby significantly improving the wind system's performance when wind and machine parameters vary.

2. MODELING OF THE MECHANICAL PART OF THE WIND TURBINE

The interaction between wind turbine blades and wind is a complex process involving physical phenomena. Wind drives turbine blades, which rotate to convert wind kinetic energy into electrical energy. The turbine's electrical energy generation is influenced by wind speed, blade size, and air density. Mathematical models describe this interaction using fluid mechanics and aerodynamics laws [8].

One of the most common expressions to describe the converted power of a wind turbine is the Betz equation, given by the following equation [8-9]:

$$P_\omega = \frac{1}{2}\rho S v_\omega^3 C_p(\lambda,\beta). \quad (2)$$

This equation states that the maximum power that can be extracted from the wind is equal to 16/27 of the kinetic power of the incident wind. This means that the turbine's converted power can never exceed this theoretical limit. This coefficient C_p is therefore very specific to the turbine considered; it depends on the variables v and Ω_t and on the parameter β. More generally, the two variables are combined to define a new λ variable called the speed ratio or "tip speed ratio" (TSR) [9,10]

$$\lambda = \frac{\Omega_t . R_t}{v_\omega}. \quad (3)$$

The following equation [9] gives the power coefficient for this kind of turbine:

$$C_p(\lambda,\beta) = 0.5\left[116\left(\frac{1}{\lambda+0.08\beta}-\frac{0.035}{\beta^3+1}\right)-0.4\beta-5\right] \exp\left[-21\left(\frac{1}{\lambda+0.08\beta}-\frac{0.0035}{\beta^3+1}\right)+0.0068\lambda\right]. \quad (4)$$

To maximize power without speed control, this method assumes that the wind speed, and consequently the rotational speed of the turbine, varies very little in steady state. This leads us to deduce from the dynamic equation of the turbine in steady state that the mechanical torque exerted on the shaft is considered to be zero in steady state [9]. Wind fluctuations are the main disturbance in the wind power conversion chain, causing power variations. To extract maximum power, techniques involve determining the turbine speed, which allows for the maximum power generated. This is evident in Fig. 3's block diagram [8].

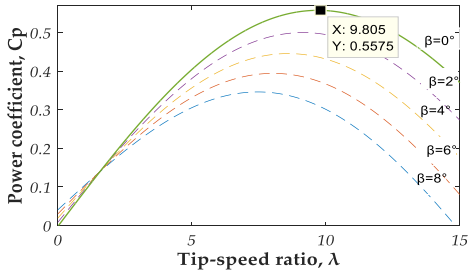

Fig. 2 – Aerodynamic power coefficient variation Cp against tip speed ratio λ and pitch angle β.

For maximum power extraction, the variable λ is assigned its optimum λ_{opt}value, corresponding to the maximum power coefficient, $C_{p\text{-}max}$. The value of the reference electromagnetic torque must then be set to the maximum value. A plot of the variation of this coefficient as a function of the specific speed λ for different values of the angle of orientation of the β blades, (Figure .3), makes it possible to have the maximum point of this coefficient ($C_{p-max} = 0.55$) which corresponds to the values optimum values ($\lambda_{opt} = 9.805$ and $\beta_{opt} = 0^\circ$)With these values, the

turbine will operate with maximum efficiency and thus provide optimum mechanical power [9-10].

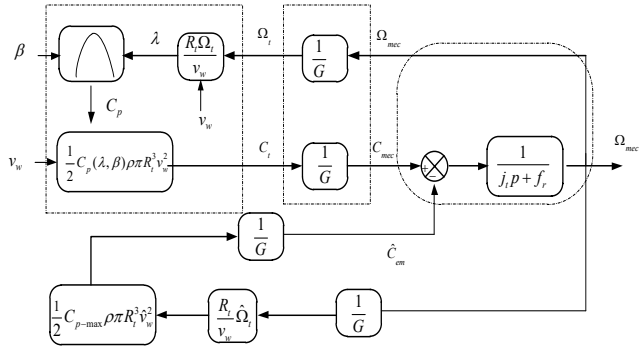

Fig. 3 – Device control without control speed.

3. **BDFIG CONTROL MODEL**

To order the BDFIG, we must have its model with a precise knowledge of the constituent elements. Mathematically [10,11], this model can be used to design and simulate control algorithms, as well as study and analyze transient regimes. Therefore, it is realistic to set conditions and assumptions for the behavioral model [11].

$$\begin{cases} v_{sp}^{d} = R_{sp} i_{sp}^{d} + \frac{d}{dt}\varphi_{sp}^{d} - \omega_{sp}\varphi_{sp}^{q} \\ v_{sp}^{q} = R_{sd} i_{sp}^{q} + \frac{d}{dt}\varphi_{sp}^{q} + \omega_{sp}\varphi_{sp}^{d} \\ v_{sc}^{d} = R_{sc} i_{sc}^{d} + \frac{d}{dt}\varphi_{sc}^{d} - (\omega_{sp} - (P_p + P_c)\omega_r)\varphi_{sc}^{q} \\ v_{sc}^{q} = R_{sc} i_{sc}^{q} + \frac{d}{dt}\varphi_{sc}^{q} + (\omega_{sp} - (P_p + P_c)\omega_r)\varphi_{sc}^{d} \\ v_{r}^{d} = R_r i_r^{d} + \frac{d}{dt}\varphi_r^{d} - (\omega_{sp} - P_p\omega_r)\varphi_r^{q} \\ v_{r}^{q} = R_r i_r^{q} + \frac{d}{dt}\varphi_r^{q} + (\omega_{sp} - P_p\omega_r)\varphi_r^{d} \end{cases} . \quad (5)$$

Flux equations [8,9- 11].

$$\begin{cases} \varphi_{sp}^{d} = L_{sp} i_{sp}^{d} + M_p i_r^{d} \\ \varphi_{sp}^{q} = L_{sd} i_{sp}^{q} + M_p i_r^{q} \\ \varphi_{sc}^{d} = L_{sc} i_{sc}^{d} + M_c i_r^{d} \\ \varphi_{sc}^{q} = L_{sc} i_{sc}^{q} + M_c i_r^{q} \\ \varphi_{r}^{d} = L_r i_r^{d} + M_c i_{sc}^{d} + M_p i_{sp}^{d} \\ \varphi_{r}^{q} = L_r i_r^{q} + M_c i_{sc}^{q} + M_p i_{sp}^{q} \end{cases} . \quad (6)$$

The electromagnetic torque equation [8,9]:

$$T_{em} = \frac{3}{2}\left[P_p M_p\left(i_{sp}^{q} i_r^{d} - i_{sp}^{d} i_r^{q}\right) - P_p M_c\left(i_{sc}^{q} i_r^{d} - i_{sc}^{d} i_r^{q}\right)\right]. \quad (7)$$

For the power winding and for the control winding [9]:

$$\begin{cases} P_{sp} = \frac{3}{2}\left(v_{sp}^{d} i_{sp}^{d} + v_{sp}^{q} i_{sp}^{q}\right) \\ Q_{sp} = \frac{3}{2}\left(v_{sp}^{q} i_{sp}^{d} - v_{sp}^{d} i_{sp}^{d}\right) \end{cases}; \begin{cases} P_{sc} = \frac{3}{2}\left(v_{sc}^{d} i_{sc}^{d} + v_{sc}^{q} i_{sc}^{q}\right) \\ Q_{sc} = \frac{3}{2}\left(v_{sc}^{q} i_{sc}^{d} - v_{sc}^{d} i_{sc}^{d}\right) \end{cases} \quad (8)$$

4. **MODELING OF CONVERTERS**

The power conversion chain consists of two back-to-back converters, one acting as a rectifier and the other as an inverter, connected by a DC link. This topology ensures bidirectional active power flow, adjusts the phase shift between network current and voltage, and regulates the DC-link voltage [8,9].

4.1 MODELING OF THE STATOR (CW) SIDE CONVERTER

The BDFIG hyper-synchronous operation uses a machine-side converter (SSC) as an inverter, controlled by the Space Vector Modulation (SVM) technique. The SSC, consisting of three independent arms with two switches, allows for voltages or currents with variable amplitude and frequency on the BDFM. The switch consists of a transistor and a diode in anti-parallel [8].

The two-level voltage inverter delivers two voltage levels ($v_{dc}/2$) or ($-v_{dc}/2$), depending on the connection function as shown in the following equation:

$$v_{xo} = \frac{v_{dc}}{2}(2S_{x1} - 1). \quad (9)$$

The phase-neutral voltages are given, as a function of the phase-to-phase voltages and the phase-midpoint voltages, by:

$$\begin{bmatrix} V_A \\ V_B \\ V_C \end{bmatrix} = \begin{bmatrix} 2 & -1 & -1 \\ -1 & 2 & -1 \\ -1 & -1 & 2 \end{bmatrix} \begin{bmatrix} S_a \\ S_b \\ S_c \end{bmatrix}. \quad (10)$$

4.2 GRID-SIDE CONVERTER MODELING AND CONTROL

The grid-side converter, also known as a voltage inverter, regulates the voltage and frequency of wind turbine electrical energy to meet distribution network standards, ensuring reliable and efficient connection to the electricity grid. It offers advanced control features to optimize wind power generation and improve grid stability, guaranteeing the quality and stability of the electricity produced [4–15].

The grid-side converter (GSC) is beneficial for active power regulation and maintaining a steady intermediate circuit voltage. It reduces reference reactive power to zero, ensuring grid quality. A three-phase SVM rectifier is constructed, divided into source, converter, and load parts. The alternating side of the inverter can be represented by the reference ***abc*** equation [8-9, 15].

$$L_f \frac{d}{dt}\begin{bmatrix} i_{fa} \\ i_{fb} \\ i_{fc} \end{bmatrix} = -R_f \begin{bmatrix} i_{fa} \\ i_{fb} \\ i_{fc} \end{bmatrix} + \begin{bmatrix} v_{fa} \\ v_{fb} \\ v_{fc} \end{bmatrix} - \begin{bmatrix} v_{sa} \\ v_{sb} \\ v_{sc} \end{bmatrix}. \quad (11)$$

The PI controller and hysteresis controller are not ideal for controlling AC signals due to their variable switching frequency. Current control in a rotating frame is based on the separation of axes, allowing independent control [9–11]. This command, applied to line voltages, decouples the control of active and reactive power. The equations governing line voltages in the frame are:

$$\begin{cases} v_{sd} = R_f i_{fd} + L_f \frac{di_{fd}}{dt} - L_f \omega_s i_{fq} + v_{fd} \\ v_{sq} = R_f i_{fq} + L_f \frac{di_{fq}}{dt} - L_f \omega_s i_{fd} + v_{fq} \\ C_{dc}\frac{d}{dt}V_{dc} = S_d i_{fd} + S_q i_{fq} \end{cases} . \quad (12)$$

4.3 BDFIG'S STATOR-FLUX-ORIENTED CONTROL STRATEGY

The wind turbine's electrical energy production can be easily controlled by establishing equations linking the stator voltages of the control winding (CW) to the active and reactive stator powers of the power winding (PW). The orientation linked to the flow of the power winding is recommended. The vector control of the BDFM with oriented BP flux supplied by the voltage inverter is presented using classic PI-type

regulators. The two-phase modeling of the BDFIG is used, orienting the reference d, q to align with the stator flux of the power winding φ_{sp}[8,9],

$$\begin{cases} \varphi_{sp}^{d} = \varphi_{sp} \\ \varphi_{sp}^{q} = 0 \end{cases}. \quad (13)$$

And the power winding stator flux equation becomes:

$$\begin{cases} \varphi_{sp}^{d} = L_{sp} i_{sp}^{d} + M_{p} i_{r}^{d} \\ 0 = L_{sd} i_{sp}^{q} + M_{p} i_{r}^{q} \end{cases} \quad (14)$$

Assuming a stable electrical network with ground voltage, a constant stator flux is achieved. Neglecting the resistance of the stator windings of a Power Supply (PW) reduces the stator voltage equations to [4–8,9]

$$\begin{cases} v_{sp}^{d} = \frac{d}{dt}\varphi_{sp}^{d} \\ v_{sp}^{q} = \frac{d}{dt}\varphi_{sp}^{q} \end{cases}. \quad (15)$$

To control the machine correctly, we must first establish the relationship between the currents and the stator voltages of the CW, which will be applied to the BDFIG [8-11].

Equation 16 represents the relationship between active and reactive power, as well as power and control currents.

$$\begin{cases} P_{sp} = \frac{3}{2} v_{sp}\left(\lambda_5 \varphi_{sp}^{q} - \lambda_4 \varphi_{r}^{q} + \lambda_3 i_{sp}^{q}\right) \\ Q_{sp} = \frac{3}{2} v_{sp}\left(\lambda_5 \varphi_{sp}^{q} - \lambda_4 \varphi_{r}^{d} + \lambda_3 i_{sp}^{d}\right) \end{cases}. \quad (16)$$

The dispersion factors are written as follows:

$$\lambda_1 = \frac{L_{sp} M_c}{L_r L_{sp} - M_p^2}, \lambda_2 = L_{sc} - \frac{L_{sp} M_c^2}{L_r L_{sp} - M_p^2}$$

$$\lambda_3 = \frac{M_c M_p}{L_r L_{sp} - M_p^2}, \lambda_4 = \frac{M_p}{L_r L_{sp} - M_p^2}, \lambda_5 = \frac{L_r}{L_r L_{sp} - M_p^2}$$

By replacing the previous expression of the fluxes with their expressions in the CW stator voltage equations, we obtain:

$$\begin{cases} v_{sc}^{d} = R_{sc} i_{sc}^{d} + \left[\frac{d}{dt}\left(\lambda_1 \varphi_{r}^{d} + \lambda_2 i_{sc}^{d}\right) - \omega_{sc}\left(\lambda_1 \varphi_{r}^{q} + \lambda_2 i_{sc}^{d} - \lambda_3 \varphi_{sp}^{q}\right)\right] \\ v_{sc}^{q} = R_{sc} i_{sc}^{q} + \left[\frac{d}{dt}\left(\lambda_1 \varphi_{r}^{q} + \lambda_2 i_{sc}^{q}\right) + \omega_{sc}\left(\lambda_1 \varphi_{r}^{d} + \lambda_2 i_{sc}^{d} - \lambda_3 \varphi_{sp}^{d}\right)\right] \end{cases} \quad (17)$$

5. CONCEPT OF INTERVAL TYPE-2 FUZZY LOGIC SETS

A type-2 fuzzy system is one where the membership functions describe its premises or consequences and contain at least one type-2 fuzzy set [12].

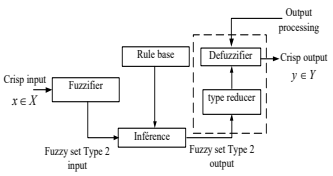

Fig. 4 – Components of an interval type-2 fuzzy system.

Fuzzy inference in this type of system results in type-2 output fuzzy sets. Interval type-2 fuzzy logic uses a fuzzy membership function, with each element's degree of membership in [0, 1]. We use Type-1 fuzzy sets to determine membership functions using real integers in the range [0, 1]. While type-1 fuzzy sets serve as a first-order approximation of uncertainty, type-2 fuzzy sets are second-order approximations [12].

Type-1 and type-2 fuzzy systems share similar structural features, including a rule base, fuzzification block, and inference mechanism. The only difference is in the output, with type-2 systems having a type reduction block before the defuzzification block.

5.1 PROPOSED DESIGN OF INTERVAL TYPE-2 FUZZY CONTROL

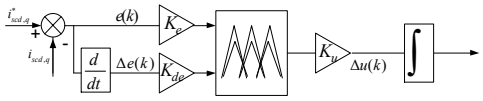

Fig. 5 – Block diagram of interval type-2 fuzzy logic regulators.

K_e:And:K_{de} are normalization gains that can be constant (or even variable).

K_u: Gain associated with the command$u(K)$.

$\Delta u(K)$: Variation of the command.

The adequate choice of the latter (K_e, K_{de} and K_u) makes it possible to guarantee the stability and to improve the dynamic and static performances of the system to be regulated [13].

To apply this control to our system, we utilized the same indirect vector control structure without a power loop, but replaced the PI controllers with type-2 fuzzy controllers. Our goal is to use this control to continuously and independently control the active and reactive powers of the flux-directed dual brushless asynchronous machine.

The controllers will be synthesized in the same way as for BDFIG's control stator currents (CW), since the first inputs will be the error between i_{sck}^{d} and its reference and its referenc ei_{sck}^{q}:

$$\begin{cases} e_{scd} = e_{sd}^{ref} - e_{scd} \\ e_{scq} = e_{sq}^{ref} - e_{scq} \end{cases} \quad (18)$$

And the variation of their errors as second inputs:

$$\begin{cases} \Delta e_{scdk} = e_{iscdk}(K) - e_{iscdk}(K-1) \\ \Delta e_{scqk} = e_{iscqk}(K) - e_{iscqk}(K-1) \end{cases} \quad (19)$$

The inputs (e and Δe) and the output (Δu) are fuzzified into seven fuzzy subsets with membership functions of a Gaussian. In our work, the interval type-2 fuzzy regulator admits seven fuzzy sets of Gaussian form for the error, the variation of the error, and the control variable, as represented in Fig. 6

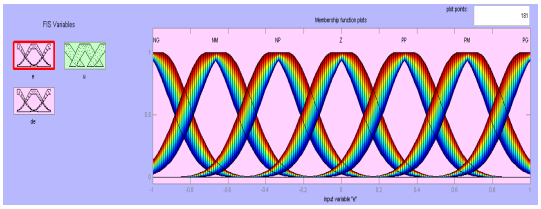

Fig. 6 – MFs of the error (e), (Δe) and (Δu) for interval type-2 FLS.

Fuzzy logic operators allow you to choose a method for processing inference. You should understand that the operator AND represents the minimum, the operator OR represents the maximum, and the operator THEN represents the maximum. The retained method will be the min/max method. Thus, based on the study of the system's behavior,

we can establish control rules that connect the output to the inputs. As mentioned, each of the two language inputs of the fuzzy controller has seven fuzzy sets, resulting in a set of forty-nine rules [13]. The inference rules represents the inference rules for our system according to Table .1

Table 1

Fuzzy rule

u		e						
		NB	NM	NS	EZ	PS	PM	PB
de	NB	NB	NB	NB	NB	NM	NS	EZ
	NM	NB	NB	NB	NM	NS	EZ	PS
	NS	NB	NB	NM	NS	EZ	PS	PM
	EZ	NB	NM	NS	EZ	PS	PM	PB
	PS	NM	NS	EZ	PS	PM	PB	PB
	PM	NS	EZ	PS	PM	PB	PB	PB
	PB	EZ	PS	PM	PB	PB	PB	PB

Figure 1 shows the complete Type 2 fuzzy logic control diagram for our system.

6. SIMULATION OUTCOMES

The paper presents simulations conducted using MATLAB/Simulink to validate control strategies for a BDFIG.

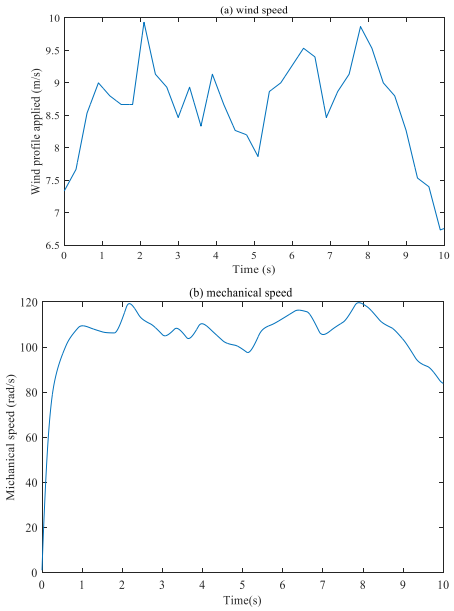

Fig. 7–(a) Wind profile applied, (b) mechanical speed.

We applied the active and reactive power control laws to the validated BDFIG model. In a practical setup, the BDFIG's control stator (CW) is connected to an inverter that utilizes a three-phase vector-controlled SVM converter as a rectifier. The rectifier control involves two loops: one is responsible for adjusting the power factor on the grid side, while the other regulates the rectified voltage to a reference value of 700V. The "MPPT" strategy controls the wind turbine-driven BDFIG to maximize captured power during low wind speeds. We determine the stator active power setpoint based on the turbine power and maintain the stator reactive power at zero to achieve a unity power factor on the stator side of the BDFIG.

Figure 7 shows the generator and wind speeds, with (b) denoting the generator speed and (a) denoting the wind speed. The simulation results show that the mechanical speed of the turbine matches the applied wind profile. The MPPT block establishes the setpoint for the stator's active power.

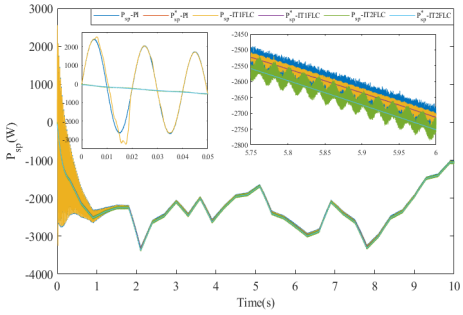

Fig. 8 – Stator (PW) active power.

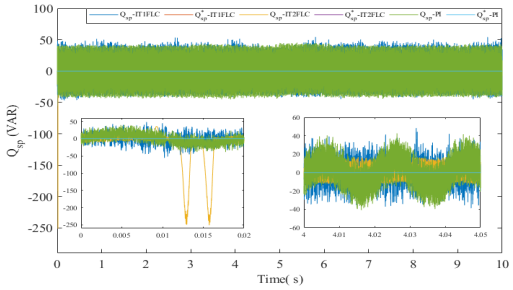

Fig. 9 – Stator (PW) reactive power.

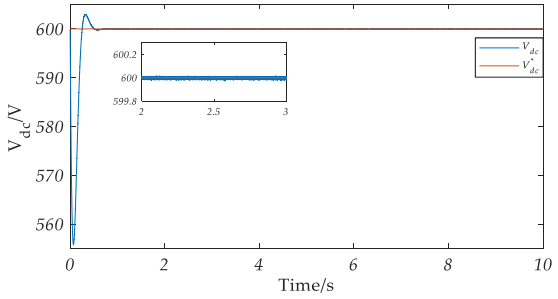

Fig. 10 – DC bus voltage.

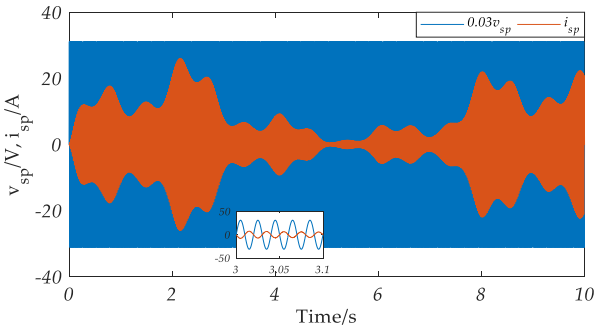

Fig. 11– The phase current and voltage of the grid.

Additional Figs. 8 and 9 examine three methods for controlling the stator's active and reactive power, based on the simulation curves in Fig. 8. The results conclude that these methods enable the active and reactive power components to be precisely distinct. Vector control with PI correctors and Type 1 FLC is advantageous for variable-speed operation; however, it is susceptible to disturbances. On the other hand, IT2FLC provides a satisfactory dynamic response, a rapid response without overshoot, and a zero static error for both active and reactive power.

During variable-speed operations, the coupling between the three powers is negligible. The active and reactive powers are maintained at the intended levels with great speed and precision by three control methods, as determined by simulations (Figs. 8, 9). However, a stuttering effect is observed. IT2FLC is more effective than vector control during a reference shift due to the absence of overshoot between the

two powers.

Figure 10 confirms the simulation of the three-phase SVM rectifier. The DC bus voltage is observed to stabilize at the command-imposed reference value. The rectifier's output DC voltage is well regulated and nearly insensitive to speed variations.

Figure 11 depicts the voltage and current of the first stator phase of the (PW) as well as their phase shift. This corresponds to the production of electrical energy with a power factor of one.

The errors are measured using three standard performance criteria: the integral of the squared error (ISE), the integral of the absolute value of the error (IAE), and the integral of time multiplied by the absolute value of the error (ITAE) [8].

Table 2.

Quantitative comparison

		VC-SVM - PI	VC-SVM - T1FLC.	VC-SVM - IT2FLC
THD (%)		1.8	1.2	0.46
Active Power	ISE	2,419*10^4	2,414*10^4	2,405*10^4
	IAE	152,1	151,4	150,9
	ITAE	272,8	272	271,8
Reactive Power	ISE	1885	1882	1304
	IAE	72,24	72,23	44,36
	ITAE	191,9	191,2	79,65

This comparison demonstrates unequivocally that VC-SVM-IT2FLC outperforms VC-SVM-PI and VC-SVM-T1FLC in terms of performance and robustness.

7. CONCLUSION

In this study, we have developed and implemented Interval Type 2 Fuzzy Logic Regulators (IT2FLC) for the control of Brushless Doubly Fed Induction Generators (BDFIG) in Wind Energy Conversion Systems (WECS). The proposed IT2FLC approach effectively addresses the challenges associated with the complex and nonlinear dynamics of BDFIGs, especially under variable wind conditions. Through extensive simulations, we have demonstrated that the IT2FLC system provides superior performance in terms of stability, robustness, and efficiency compared to traditional control methods. The ability of IT2FLR to manage uncertainties and adapt to changing operating conditions ensures optimal power extraction and efficient energy conversion, even in the presence of noisy or imprecise data. The findings of this study suggest that IT2FLC offers a promising solution for enhancing BDFIG control and performance in WECS, thereby contributing to the more reliable and efficient integration of wind energy into the electrical grid.

CREDIT AUTHORSHIP CONTRIBUTION STATEMENT

HELLALI Lallouani: Writing – review & editing, Writing – original draft, Visualization, Methodology, Formal analysis, Conceptualization.
MOUSSA Oussama: Writing – review & editing, Writing – original draft, Visualization.
BOUZIDI Ali: Visualization, Methodology, Formal analysis.
AKKA Ali**:** Visualization, Formal analysis.

Received on 22 September 2024

APPENDIX

PROTOTYPE BDFIG electrical parameters for simulation [8,9].

Power winding (PW)		Control winding (CW)	Rotor
Resistance Ω	$R_{sp} = 1.732$	$R_{sc} = 1.079$	$R_r = 0.473$
Self-inductance (mH)	$L_{sp} = 714.8$	$L_{sc} = 121.7$	$L_r = 132.6$
Mutual inductance (mH)	$M_p = 242.1$	$M_c = 59.8$	

REFERENCES

1. L. Hou, J. Ma, W. Wang, *Sliding mode predictive current control of permanent magnet synchronous motor with cascaded variable rate sliding mode speed controller*. IEEE Access, **10**, pp. 33992–34002 (2022).
2. G. Dauksha and G. Iwanski, *Indirect torque control of a cascaded brushless doubly-fed induction generator operating with unbalanced power grid*. IEEE Transactions on Energy Conversion, **35**, *2*, pp. 1065–1077 (2020).
3. R. Wang, L. Han, B. Wang, N. Yang, P. Zhao, and L. Yan, *Study of Integrated Vector Control for Brushless Doubly-Fed Machine*. In 2019 22nd International Conference on Electrical Machines and Systems (ICEMS), pp. 1–5. IEEE (2019).
4. X. Li, T. Peng, H. Dan, G. Zhang, M. Rivera, *A modulated model predictive control scheme for the brushless doubly fed induction machine*. IEEE Journal of Emerging and Selected Topics in Power Electronics, **6**, *4*, pp. 1681–1691 (2018).
5. P. Han, M. Cheng, Z. Zhang, P. Peng, *Spiral vector modeling of brushless doubly-fed induction machines with short-circuited rotor windings*. Chinese Journal of Electrical Engineering, **7,** *3*, pp. 29–41 (2021).
6. S. Bayhan, P. Kakosimos, M. Rivera, *Predictive torque control of brushless doubly fed induction generator fed by a matrix converter*. In 2018 IEEE 12th International Conference on Compatibility, Power Electronics and Power Engineering (CPE-POWERENG 2018), pp. 1–6. IEEE (2018).
7. H.M. Hesar, H.A. Zarchi, G.A. Markadeh, *Modeling and dynamic performance analysis of brushless doubly fed induction machine considering iron loss*. IEEE Transactions on Energy Conversion, **35**, *1*, pp. 193–202 (2019).
8. O. Moussa, R. Abdessemed, S. Benaggoune, H. Benguesmia, *Sliding mode control of a grid-connected brushless doubly fed induction generator*. European Journal of Electrical Engineering, **21**, *5*, pp. 421–430 (2019).
9. O. Moussa, R. Abdessemed, S. Benaggoune, *Super-twisting sliding mode control for brushless doubly fed induction generator based on WECS*. International Journal of System Assurance Engineering and Management, **10**, pp. 1145–1157 (2019).
10. S. Hu, G. Zhu, *Enhanced control and operation for brushless doubly-fed induction generator based wind turbine system under grid voltage unbalance*. Electric Power Systems Research, **207**, p. 107861 (2022).
11. J. Huang, S. Li, *Analytical expression for LVRT of BDFIG with enhanced current control to CW and reactive power support from GSC*. International Journal of Electrical Power & Energy Systems, **98**, pp. 243–255 (2018).
12. L. Hellali, S. Belhamdi, *Performances of type 2 fuzzy logic control based on direct torque control for double star induction machine*. Rev. Roum. Sci. Techn. – Electrotechn. et Energ., **65**, *1–2*, pp. 103–108 (2020).
13. O. Moussa, L. Hellali, S. Belhamdi, *Direct torque control with space vector modulation using interval type-2 fuzzy logic regulators of dual star induction machine fed by two three-level neutral point clamped inverter*. Rev. Roum. Sci. Techn. – Électrotechn. et Énerg., **69**, *2*, pp. 159–164 (2024).
14. I. Yaichi, A. Semmah, P. Wira, *Control of doubly fed induction generator using artificial neural network controller*. Revue Roumaine des Sciences Techniques – Série Électrotechnique et Énergétique, **68**, *1*, pp. 46–51 (2023).
15. F. Amrane, A. Chaiba, B. Francois, *Improved adaptive nonlinear control for variable speed wind-turbine fed by direct matrix converter*. Revue Roumaine des Sciences Techniques – Série Électrotechnique et Énergétique, **68**, *1*, pp. 58–64 (2023).